

# Transport properties of nano-devices: a one dimensional model study

Zhongxi Zhang, C. F. Destefani, Chris McDonald, and Thomas Brabec  
*Center for Photonics Research, University of Ottawa, Ottawa, K1N 6N5 ON, Canada*  
(Dated: November 20, 2018)

A 1D model study of charge transport in nano-devices is made by comparing multi-configuration time dependent Hartree-Fock and frozen core calculations. The influence of exchange and Coulomb correlation on the tunneling current is determined. We identify the shape of the tunneling barrier and the resonance structure of the nano-device as the two dominant parameters determining the electron transport. Whereas the barrier shape determines the size of the tunneling current, the resonances determine the structure of the current.

PACS numbers: 73.63.-b, 73.23.Hk, 05.60.Gg

Nano-systems have been receiving great attention lately, mainly because of two reasons. First, they allow the realization of nano-scale electronic devices, such as Coulomb blockade structures, transistors, diodes, and switching devices.<sup>1,2,3,4,5,6,7</sup> Second, transport properties are governed by quantum mechanics, which opens a novel venue for investigating fundamental transport properties of quantum few-/many-body systems. The theoretical description of quantum transport properties has proven to be a true challenge. Conventional theories, such as the Landauer-Buttiker approach and density functional theory do not perform well,<sup>8,9,10,11,12</sup> and are orders of magnitude off the experimentally measured currents. Recently, configuration-interaction (CI) analysis was shown to give a much better agreement,<sup>13</sup> with currents about three times the experimental values.

Despite this progress, the physics underlying electron transport in nano-devices is not yet well understood. Here, a first step is made to close this gap. Our analysis is based on a one dimensional multi-configuration time-dependent Hartree-Fock (MCTDHF) method<sup>14</sup>. The MCTDHF approach takes full account of exchange and correlation effects. Whereas in CI the basis is fixed and only the expansion coefficients are optimized, in MCTDHF both coefficients and basis functions are optimized. As a result, a much smaller basis set can be used. This proves important especially for transport processes in continuum-like structures, where a CI analysis requires a large number of basis functions for convergence.

The influence of many-body effects on transport phenomena presents a central issue in the characterization of nano-devices. We use the following approach to investigate this question. The MCTDHF analysis is compared to time-dependent Hartree-Fock (TDHF), frozen-core Hartree-Fock (FCHF) and frozen core Hartree (FCH) calculations. Comparison of the different approaches reveals the role of exchange and correlation in the electron transport. It also gives a sense of the quality of various approximations used in the electron transport analysis of nano-devices. Further, a correlation measure is introduced with the goal to quantify the influence of many-body effects. Finally, we identify two parameters that determine the tunneling characteristics, namely, the shape of the barrier and the resonance structure of the nano-

device.

A schematic of the 1D model potential  $U(x)$  of the nano-device is given in Fig. 1. The potential is determined by  $U(x) = U_0$  for  $|x| \leq l$  and  $U(x) = V_{nd}(x) + V_c(x)$  otherwise. Atomic units are used throughout the paper, where 1 bohr = 0.0529 nm, 1 hartree = 27.2 eV, and  $i_0 = 6.6 \times 10^{-3}$  A is the atomic unit of current. The parameter  $U_0$  represents the depth of the nano-device and its length is  $2l$ . We assume that the device is neutral, i.e., it contains the same number of ions and electrons,  $f_c = 4$ . Therefore, for  $|x| > l$ ,  $U(x)$  is composed of the ion potential  $V_{nd}(x) = -\sum_{i=1}^{f_c} 1/\sqrt{a_n^2 + (x - d_i)^2}$ , and of the effective conductor potential,  $V_c(x) = U_f[2 - \tanh((d + x)/w) - \tanh((d - x)/w)]/2$ . Here  $d_i$  is the position of the  $i$ th nucleus,  $a_n$  is the shielding parameter of the 1D ion potential, and  $U_f$  is the effective potential in the conductor. Parameters  $d$  and  $w$  are used to model the potential in the transition region between nano-device and metal<sup>15</sup>.

Further the Coulomb interaction between the  $f = f_c + 1$  electrons is modelled by  $(1/2) \sum_{i,j}^f V_{ee}(x_i, x_j)$  with  $V_{ee}(x_i, x_j) = 1/\sqrt{a^2 + (x_i - x_j)^2}$ . The shielding parameter  $a$  removes the Coulomb singularity. As the averaging over the dimensions transversal to the direction of electron transport results in an effective, shielded Coulomb interaction,  $a$  can be viewed to represent the transversal properties of the nano-device<sup>16</sup>.

For all the calculations presented here the number of electrons is fixed to  $f = 5$ , four core electrons in the nano-device plus one electron tunneling through the device. The wavefunction of the transport electron is given by a Gaussian initial wavepacket,  $\varphi_t$ , with  $1/e$ -width  $\alpha$ , momentum  $p_0$ , and energy  $E_0 = p_0^2/2$ , see Fig. 1). The initial distance from the tunneling device,  $x_0 = -200$  bohr, is chosen large enough so that the total multi-electron initial wavefunction can be written as an anti-symmetrized tensor product of the electronic ground state of the nano-device,  $\Psi_c$ , and of the transport electron, i.e.,  $\Psi = \mathcal{A}[\Psi_c(q_1, q_2, q_3, q_4) \otimes \varphi_t(q_5)]$ . Here,  $\mathcal{A}$  denotes the anti-symmetrization operator, and  $q_i = (x_i, s_i)$  ( $i = 1, \dots, 5$ ) the space-spin coordinate.

The MCTDHF current is a combination of various single and multi-electron processes. To untangle the different contributions and their importance we calculate the

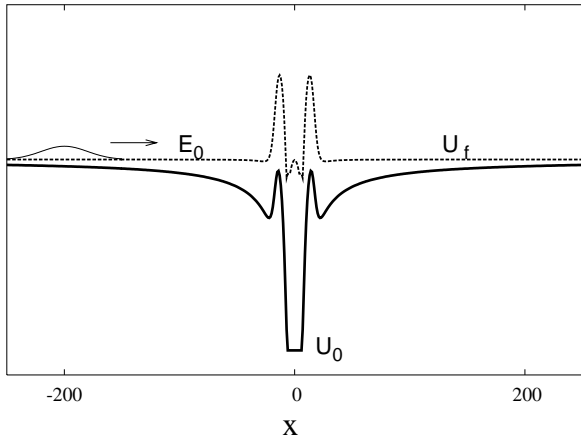


FIG. 1: The effective ion potential  $U(x)$  (thick solid), the initial Gaussian wavepacket (thin solid), and the effective frozen Hartree potential  $u_{eff}^{FCH}(x) = U(x) + u^{FCH}(x)$  (dashed). The Coulomb potential  $u^{FCH}(x)$  is the Hartree contribution of the initial core.

electron transport by different methods. In the MCTDHF approach the exact wavefunction is approximated by the ansatz

$$\Psi = \frac{1}{\sqrt{f!}} \sum_{j_1, \dots, j_f}^n A_{j_1 \dots j_f}(t) \varphi_{j_1}(q_1, t) \dots \varphi_{j_f}(q_f, t). \quad (1)$$

Note that the number of wavefunctions  $n$  in the ansatz is larger than the number of electrons, resulting in  $\binom{n}{f}$  Slater determinants. The ansatz is inserted into the Schrödinger equation and the Dirac-Frenkel variational method is used to derive a coupled system of time-dependent, nonlinear, partial differential equations for the coefficients  $A$  and wavefunctions  $\varphi$ . For more information on the MCTDHF method, see Ref. 14. In the calculations the simulation interval is chosen from  $x = -400$  bohr to  $x = 400$  bohr with the number of grid points  $N = 800$ . Convergence is obtained for  $n = 11$  wavefunctions. Increasing  $n$  and  $N$  changes the electron density by less than 0.1%.

The second method used in our investigation is time-dependent Hartree Fock (TDHF), which is MCTDHF for  $f = n$ . The third and fourth methods are frozen core methods, where the correlated ground state wavefunction of the nano-device is calculated by MCTDHF and assumed to remain frozen during the transport of the conducting electron. In dependence on whether exchange effects between ground state and conducting electron are taken into account, these approaches are termed frozen core Hartree (FCH) and frozen core Hartree Fock (FCHF). The frozen core approximation reduces the multi-electron Schrödinger equation to a single-electron

equation given by

$$\begin{aligned} i\partial_t \phi(x, t) = h\phi(x, t) + \int V_{ee}(x', x)\rho_c(x')dx'\phi(x, t) \\ - \int \Gamma_c^{(1)}(q'|q)V_{ee}(x', x)\phi(x', t)\delta_{s,s'}dq' \\ - \int \Gamma_c^{(1)}(q'|q)h(x')\phi(x', t)\delta_{s,s'}dq' \\ - 2 \int \Gamma_c^{(2)}(q', q''|q', q)V_{ee}(x', x'')\phi(x'', t)\delta_{s,s''}dq'dq'', \end{aligned} \quad (2)$$

where  $s$  is the spin index of the conducting electron,  $\rho_c(x) = \int \Gamma_c^{(1)}(q|q)ds$ , and  $h = p^2/2 + U(x)$ . The core electron reduced density matrices are defined as  $\Gamma_c^{(1)}(q'_1|q_1) = [2/(f_c - 1)] \int \Gamma_c^{(2)}(q'_1, q_2|q_1, q_2)dq_2$  and  $\Gamma_c^{(2)}(q'_1, q'_2|q_1, q_2) = \binom{f_c}{2} \int \Psi_c^*(q'_1, q'_2, q_3, \dots, q_{f_c})\Psi_c(q_1, q_2, q_3, \dots, q_{f_c})dq_3 \dots dq_{f_c}$ <sup>17</sup>. The first two terms on the right hand side of Eq. (2) give the frozen core Hartree (FCH) approximation. The last three terms account for the ground state correlation of the nano-device and the exchange effect between bound and tunneling electrons. In order to keep the problem as simple as possible, we focus here on the field-free scattering of the electron from the nano-device. In the weak field limit, where the field induced distortion of the bound state is weak, the change of the initial energy of the incoming electron  $E_0$  is equivalent to applying a bias voltage  $V \approx E_0$  determined by the chemical potential of the two leads. One atomic units of energy change corresponds to a bias change of 27.2V.

In Figs. 2 and 3 we have plotted the average current  $I$  flowing through the nano-device as a function of the energy of the incoming electron. The parameters have been chosen to reflect experimental systems, see the figure caption. The device size of around 0.5 nm, the ionization potential of 10 eV, and the Fermi energy of -5eV are typical values found in experimental nano-molecule systems, such as in the Au/dithiolated-benzene/Au junction<sup>11</sup>. The average current  $I(x) = \langle \tilde{i}(x, t) \rangle$  is calculated between the initial time and the time when the reflected pulse returns to its initial position. The time dependent tunneling current  $\tilde{i}(x, t)$  is obtained by

$$\begin{aligned} \tilde{i}(x, t) = \frac{f}{2i} \\ \times \sum_{j,k}^n \tilde{\rho}_{j,k} [\varphi_j^*(x, t)\partial_x \varphi_k(x, t) - \varphi_k^*(x, t)\partial_x \varphi_j(x, t)], \end{aligned} \quad (3)$$

where  $\tilde{\rho}_{j,k} = \sum_{i_2, \dots, i_f}^n A_{j, i_2 \dots i_f}^* A_{k, i_2 \dots i_f}$  denotes the density matrix and  $I(x)$  is calculated at  $x = 80$  bohr. The electron energy  $E_0$  is measured with reference to  $U_f$ .

The major difference between Figs. 2 and 3 is the use of different shielding parameters  $a = 4.5$  bohr and  $a = 3.0$  bohr, respectively. The decreasing value of  $a$  reflects an increasing electron-electron interaction strength. Although it is difficult to assign the 1D Coulomb correlation

strength resulting from different values of  $a$  to specific devices, some qualitative considerations can be made. We believe that  $a \approx 2$  to 5 represents best the 3D experimental situation. On the one hand, calculations for  $a = 7$  show hardly any interaction between the transport and the core electrons. On the other hand, for  $a < 2$ , the electron repulsion becomes too strong. As a result, the ionization potential increases and can no longer be fitted to values typical of experimental devices.

The MCTDHF, TDHF, and FCHF results are depicted by the full, dotted, and dashed lines, respectively. The dash-dotted line in Fig. 2 represents the FCH result. All curves show the same general trend. Whereas the structure of the curves is determined by the resonances, their growth with increasing  $E_0$  depends mainly on the height and thickness of the tunneling barrier. There are two resonances in the ranges  $E_0 = 0.02 \sim 0.04$  and  $E_0 = 0.1 \sim 0.14$ . The strength and width of the second resonance is more pronounced mainly due to the weaker tunneling barrier for higher  $E_0$ .

The comparison of the various approaches reveals the role of exchange and correlation effects in determining the current through the model nano-system. The FCH approach neglects two important effects: (i) exchange interaction between conducting and bound electrons; (ii) interaction between tunneling and core electrons in the sense that the tunneling electron induces a perturbation to the bound electrons of the nano-system. The resulting potential change modifies the tunneling current. In order to capture this effect, the frozen core approximation has to be removed. In the FCHF approximation the exchange interaction is taken into account, whereas approximation (ii) remains. In the TDHF approach part of the limitation (ii) is removed by making the wavefunction, that governs the bound electron dynamics, time-dependent. However, TDHF does still not fully account for the cross-talk between conduction and bound electrons, as correlation is neglected by the product ansatz of single-electron wavefunctions. Finally, in MCTDHF all effects are treated properly.

Figure 2 shows that FCH introduces a significant error with regard to the position of the resonances, as can be seen from the first resonance. As a result of the large width of the second resonance, the difference between FCH and MCTDHF is blurred. In Fig. 3, FCH was not plotted as the error in resonance position becomes of the order of the difference between first and second resonances. Comparison of FCH and FCHF in Fig. 2 shows that a substantial part of the resonance shift comes from the neglect of the exchange effect.

The remaining difference can be attributed to the perturbation of the electrons in the nano-device caused by the tunneling electron. The resulting change of the electronic core modifies the position of the resonances and therewith the tunneling current. A comparison of the FCHF, TDHF and MCTDHF in Fig. 3 demonstrates the importance of correlation in the interaction between bound and tunneling electrons<sup>18</sup>. Although the TDHF

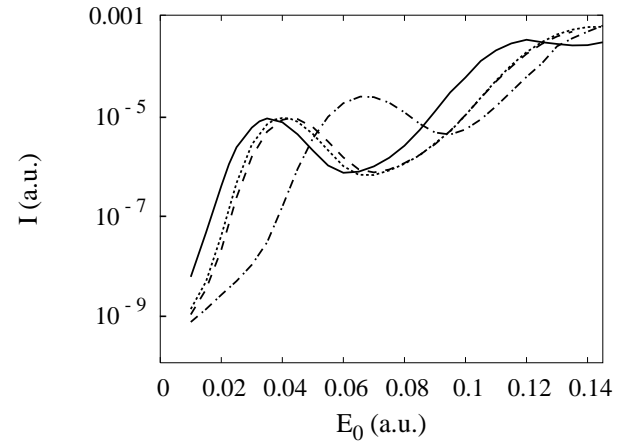


FIG. 2: Average current versus energy  $E_0$ , obtained by MCTDHF (full), TDHF (dotted), FCHF (dashed), and FCH (dash-dotted). Parameters are:  $f_c = 4$ ,  $a = 4.5$  bohr,  $2l = 10$  bohr,  $d = 11.0$  bohr,  $w = 0.8$  bohr,  $\alpha = 40$  bohr,  $x_0 = -200$  bohr,  $U_0 = -0.92$  hartree,  $U_f = -0.18$  hartree (-5 eV), and  $I_p = 0.382$  hartree (10.4 eV).

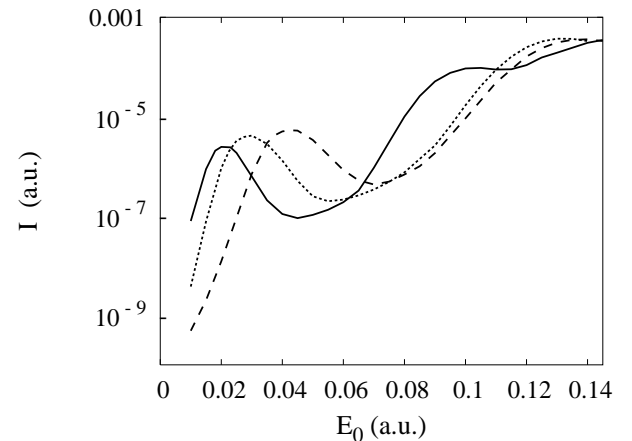


FIG. 3: Average current versus energy  $E_0$ , obtained by MCTDHF (full), TDHF (dotted), and FCHF (dashed). Parameters are the same as those given in Fig. 2, except for  $a = 3.0$  bohr. The following parameters had also to be modified to keep the ionization potential  $I_p = 0.388$  hartree (10.6 eV) and resonance structure as close as possible to the system in Fig. 2:  $2l = 12$  bohr, and  $U_0 = -0.97$  hartree.

approach performs better than FCHF, it is in most places off by an order of magnitude from the MCTDHF calculation. This highlights the fact that during tunneling a highly correlated state between core and transport electrons builds up. The amount of correlation strongly depends on the electron-electron interaction strength, as can be seen from a comparison between Figs. 2 and 3.

Finally, over most of the energy range ( $E_0 \leq 0.12$ ) the electron transport is elastic. The nano-device returns to its ground state after the conducting electron has passed.

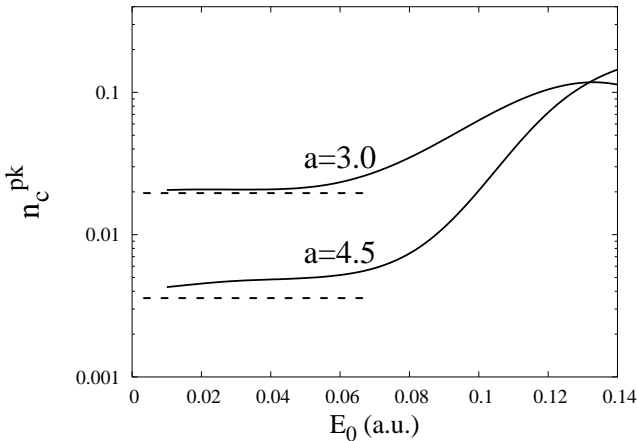


FIG. 4: Dashed lines: correlations of the initial bound states,  $n_c(a, t = 0)$ . Solid curves: overall correlations measured at the tunneling peak of the nano-devices,  $n_c^{pk}(a)$ , the peak value of  $n_c(a, t)$ . The difference between solid and dashed lines is the contribution due to the interaction between tunneling and core electrons.

Only for energies ( $E_0 > 0.12$ ) we find evidence of excited state population. The excitation causes a suppression of the resonance at  $E_0 = 0.12$  in Fig. 2. This "strong-field"

limit is not analyzed further here.

One way to characterize the build up of Coulomb correlation between tunneling and bound electrons is to consider the occupation number of the natural orbitals, which are the eigenvalues of the density matrix  $\tilde{\rho}$ <sup>17</sup>. The number of natural orbitals is  $n > f$  and they are ordered with respect to their eigenvalue. The lowest orbital refers here to the largest occupation number. In the uncorrelated HF limit only the lowest  $f$  orbitals are occupied. Therefore the Coulomb correlation can be measured by  $n_c(a, t) = \sum_{i=f+1}^n \lambda_i(a, t)/f$ , which is the occupation number of the natural orbitals with  $i > f$ . Here,  $\sum_{i=1}^n \lambda_i(a, t) = f \lambda_i(a, t) > \lambda_{i+1}(a, t)$ , and  $0 \leq n_c(a, t) \leq 1 - f/n$ .

The correlation measure is plotted in Fig. 4 for the parameters of Figs. 2 and 3. Up to  $E_0 \approx 0.06$  the correlation introduced by the tunneling electron is smaller than the initial core correlation  $n_c(a, t = 0)$ , which is independent of the value of  $E_0$ . In this range the physics is dominated by the bound electrons that determine the position of the resonances. For larger energies, the interaction between bound electrons and tunneling electron adds a significant amount of correlation to the system. The sharp increase of  $n_c(a, t)$  agrees with the large difference between MCTDHF and the other approaches in Figs. 2 and 3.

---

<sup>1</sup> D. Porath and O. Milo, *J. Appl. Phys.* **81**, 2241 (1997).  
<sup>2</sup> H. Park, J. Park, A. K. L. Lim, E. H. Anderson, A. P. Alivisatos, and P. L. McEuen, *Nature (London)* **407**, 57 (2000).  
<sup>3</sup> M. DiVentra, S. T. Pantelides, and N. D. Lang, *Appl. Phys. Lett.* **76**, 3448 (2000).  
<sup>4</sup> E. W. Wong, C. P. Collier, M. Behloradsky, F. M. Raymo, J. F. Stoddart, and J. R. Heath, *J. Am. Chem. Soc.* **122**, 5831 (2000).  
<sup>5</sup> J. Chen, M. A. Reed, A. M. Rawlett, and J. M. Tour, *Science* **286**, 1550 (1999).  
<sup>6</sup> M. DiVentra, S. G. Kim, S. T. Pantelides, and N. D. Lang, *Phys. Rev. Lett.* **86**, 288 (2001).  
<sup>7</sup> W. Tain, S. Datta, S. Hong, R. Reifenberger, J. I. Henderson, and C. P. Kubiak, *J. Chem. Phys.* **109**, 2874 (1998); L. E. Hall, J. R. Reimers, N. S. Hush, and K. Silverbrook, *ibid.* **112**, 1510 (2000); E. G. Emberly and G. Kirczenow, *Phys. Rev. B* **58**, 10911 (1998).  
<sup>8</sup> N. D. Lang and Ph. Avouris, *Phys. Rev. Lett.* **84**, 358 (2000); M. DiVentra, S. T. Pantelides, and N. D. Lang *ibid.* **84**, 979 (2000).  
<sup>9</sup> J. Taylor, H. Guo, and J. Wang, *Phys. Rev. B* **63**, 245407 (2001).  
<sup>10</sup> P. S. Damle, A. W. Ghosh, and S. Datta, *Phys. Rev. B* **64**, 201403(R) (2001).  
<sup>11</sup> M. A. Reed, C. Zhou, C. J. Muller, T. P. Burgin, and J. M. Tour, *Science* **278**, 252 (1997); A. Nitzan and M. A. Ratner, *Science* **300**, 1384 (2003).  
<sup>12</sup> C. Toher, A. Filippetti, S. Sanvito, and K. Burke, *cond-mat/0506244*.  
<sup>13</sup> P. Delaney and J. C. Greer, *Phys. Rev. Lett.* **93**, 036805 (2004).  
<sup>14</sup> J. Zanghellini, M. Kitzler, T. Brabec, and A. Scrinzi, *J. Phys. B* **37**, 763 (2004); J. Caillat, J. Zanghellini, M. Kitzler, O. Koch, W. Kreuzer, and A. Scrinzi *Phys. Rev. A* **71**, 012712 (2005). M. Kitzler, J. Zanghellini, Ch. Jungreuthmayer, M. Smits, A. Scrinzi, and T. Brabec, *Phys. Rev. A* **70**, 041401(R) (2004).  
<sup>15</sup> N. D. Lang, *Phys. Rev. B* **45**, 13599 (1992).  
<sup>16</sup> P. I. Tamborenea and H. Metiu, *Phys. Rev. Lett.* **83**, 3912 (1999); A. J. Fendrik, M. J. Sanchez, and P. I. Tamborenea, *Phys. Rev. B* **63**, 115313 (2001).  
<sup>17</sup> P. Löwdin, *Phys. Rev.* **97**, 1474 (1955); R. G. Parr and Weitao Yang *Density-Functional Theory of Atoms and Molecules* (Oxford Science Publications 1989).  
<sup>18</sup> N. Sai, M. Zwolak, G. Vignale, and M. Di Ventra, *Phys. Rev. Lett.* **94**, 186810 (2005).